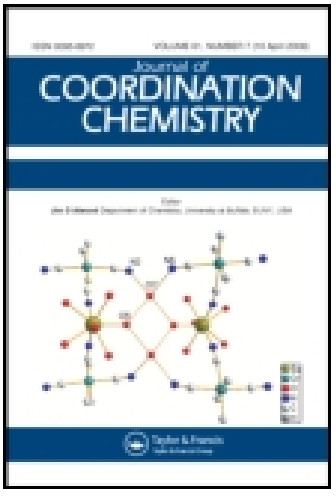

Journal of Coordination Chemistry
Publication details, including instructions for authors and subscription information:
http://www.tandfonline.com/loi/gcoo20

Ligational behavior of S, N, and O donor quinoxaline derivatives toward the later first-row transition metal ions

Naveen V. Kulkarni [a], Nagaraj H. Bevinahalli [a] & Vidyanand K. Revankar [a]

[a] Department of Studies in Chemistry, Karnatak University, Pavatenagar, Dharwad 580003, Karnataka, India

Published online: 11 Jun 2010.

To cite this article: Naveen V. Kulkarni, Nagaraj H. Bevinahalli & Vidyanand K. Revankar (2010) Ligational behavior of S, N, and O donor quinoxaline derivatives toward the later first-row transition metal ions, Journal of Coordination Chemistry, 63:10, 1785-1794, DOI: 10.1080/00958972.2010.487938

To link to this article: http://dx.doi.org/10.1080/00958972.2010.487938

Journal of Coordination Chemistry
Vol. 63, No. 10, 20 May 2010, 1785–1794

Ligational behavior of S, N, and O donor quinoxaline derivatives toward the later first-row transition metal ions

NAVEEN V. KULKARNI, NAGARAJ H. BEVINAHALLI and VIDYANAND K. REVANKAR*

Department of Studies in Chemistry, Karnatak University, Pavatenagar, Dharwad 580003, Karnataka, India

(*Received 30 November 2009; in final form 8 February 2010*)

Ligands derived from quinoxaline-2,3-(1,4H)-dithione are treated with Co(II), Ni(II), Cu(II), and Zn(II) chlorides to yield stable complexes. The prepared compounds are characterized by spectro-analytical techniques and magnetic susceptibility measurements, and the coordination behavior of ligands is discussed. All the complexes are octahedral and mononuclear with general formula $[MLCl_2(H_2O)]$. The electrochemical behavior of the synthesized compounds was investigated by cyclic voltammetry studies and the redox activity is explained.

Keywords: Coordination compound; Quinoxaline-2,3-(1,4H)-dithione; Quinoxaline-2,3-(1,4H)-dione; Isatin

1. Introduction

In coordination chemistry, ligational behavior of multidentate ligands, especially with different donors is of interest. A coordination cavity created by oxygen, nitrogen, and sulfur donors can provide a better fit in terms of size and flexibility for transition metal(II) ions. Structural features (stereochemical arrangement) of a heterocyclic or acyclic core molecule which contain these donors play an important role in the coordination behavior [1]. Metal complexes derived from the S, N, and O donor ligands are of interest because of their versatile structural and functional properties, and their applications in biochemistry, catalysis, medicine, and material research [2–4]. The task of constructing bicompartmental SNO donor ligands and their complexes is of immense interest.

Quinoxaline derivatives are a very important class of nitrogen-containing compounds and have been widely used in dyes [5], pharmaceuticals [6, 7], and electrical/photochemical materials [8–10]. In particular, thione-substituted quinoxaline derivatives show applications in medicinal chemistry.

In this work, we select quinoxaline-2,3-(1,4H)-dithione for construction of ligand systems. One of the two thione functionalities was replaced by the hydrazine sidearm

*Corresponding author. Email: vkrevankar@rediffmail.com

Journal of Coordination Chemistry
ISSN 0095-8972 print/ISSN 1029-0389 online © 2010 Taylor & Francis
DOI: 10.1080/00958972.2010.487938

and is used for condensation with the ketone-functionality of isatin and quinoxaline-dione. One of the two ketonic groups of isatin and quinoxaline-dione interacts with the hydrazine sidearm and constructs L^1 and L^2, respectively (figure 1). The free thione group of quinoxaline and the free ketonic oxygen of isatin, and another quinoxaline ring along with the nitrogen constitute the SNO cavity. Hence, formed ligands interact with later first-row transition metal chlorides to yield complexes. The compounds are characterized by the spectro-analytical techniques and the electrochemical behavior was investigated.

2. Experimental

2.1. *Reagents and apparatus*

The chemicals used were of reagent grade. Purified solvents were used for the synthesis of ligands and complexes. Syntheses of quinoxaline-2,3-(1,4H)-dione [11] and quinoxaline-2,3-(1,4H)-dithione [12] were done according to the literature with slight modification. Isatin was purchased from Sigma Aldrich and the metal chlorides {$CoCl_2 \cdot 6H_2O$, $NiCl_2 \cdot 6H_2O$, $CuCl_2 \cdot 2H_2O$, and $ZnCl_2$} were used for the complex formation. C, H, N, and S analyses were carried out on a ThermoQuest elemental analyzer. Metal and chloride estimations were done by standard procedures after decomposition in nitric acid [13]. Molar conductivity measurements in dimethylformamide (DMF) were made on an ELICO-CM-82 conductivity bridge with a conductivity

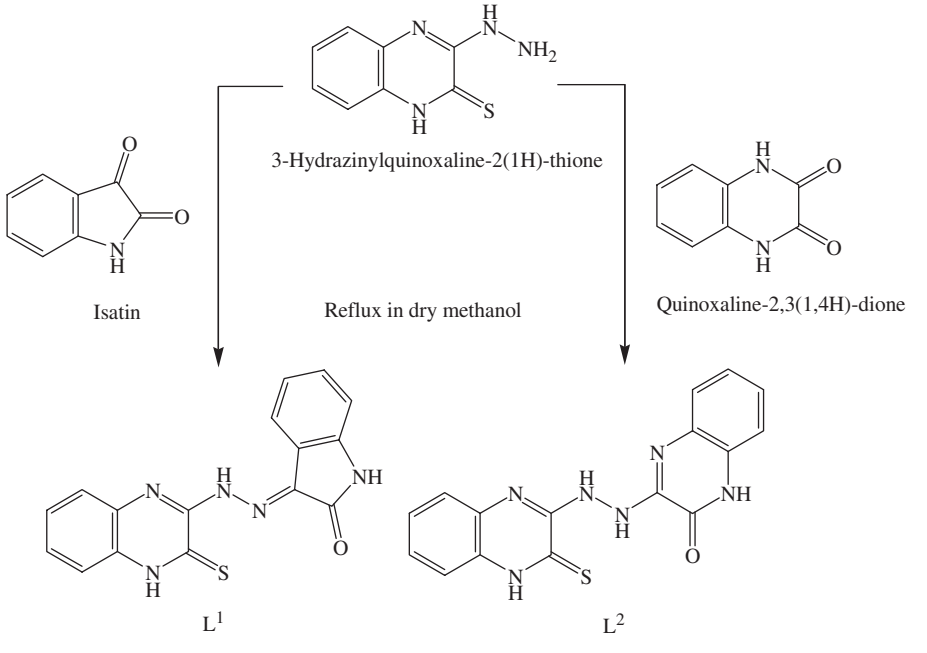

Figure 1. Schematic representation of preparation of ligands.

cell having cell constant $0.51\,cm^{-1}$. Magnetic susceptibility measurements were made using a Faraday balance at room temperature with $Hg[Co(SCN)_4]$ as calibrant. ^{1}H-NMR spectra were recorded in DMSO-d_6 on a Bruker-300 MHz spectrometer at room temperature using tetramethylsilane (TMS) as internal reference. Infrared (IR) spectra were recorded in KBr using an Impact-410 Nicolet (USA) FT-IR spectrometer from 4000 to $400\,cm^{-1}$. Electronic spectra of the complexes were recorded on a Hitachi 150–20 from 1000–200 nm. Cyclic voltammetric studies were performed at room temperature in DMF under pure nitrogen with a CHI1110A electrochemical analyzer (USA) comprising a three electrode assembly of glassy carbon working electrode, platinum auxiliary electrode, and non-aqueous $Ag^+/AgCl$ reference electrode. Tetramethylammonium chloride ($0.01\,mol\,L^{-1}$) was used as supporting electrolyte and the instrument was standardized by ferrocene/ferrocenium redox couple. Electron spin resonance (ESR) of the copper complexes was carried out on a Varian E-4X-band electron paramagnetic resonance (EPR) spectrometer using tetracyanoethylene (TCNE) as the g-marker. Fast atom bombardment (FAB) mass spectra were recorded from a JEOL SX 102/DA-6000 mass spectrometer using Argon/Xenon (6 kV, 10 mA) as the FAB gas and *m*-nitrobenzyl alcohol as matrix. Thermogravimetric (TG) and differential thermal analysis (DTA) measurements of the complexes were recorded in nitrogen on a Universal V2 4F TA instrument at $10^\circ C\,min^{-1}$ and scan range of 25–800°C.

2.2. *Synthesis*

2.2.1. Synthesis of 3-hydrazinoquinoxaline-2-thione. Hydrazine hydrate in methanol (0.6 mL, $0.1\,mol\,L^{-1}$) is added dropwise to a methanolic solution of quinoxaline-2,3-(1,4H)-dithione (1.94 g, $0.1\,mol\,L^{-1}$) with constant stirring. The mixture is then refluxed for 2 h over a steam bath. The product formed as a shining dark yellow solid was filtered, thoroughly washed with methanol, and then air dried (Yield: 83%, m.p.: 182–184°C) (figure 2).

2.2.2. Synthesis of L^1 and L^2. To a hot dry methanolic solution of 3-hydrazinoquinoxaline-2-thione (1.92 g, $0.1\,mol\,L^{-1}$), a hot methanolic solution of isatin (1.51 g, $0.1\,mol\,L^{-1}$) or quinoxaline-2,3(1,4H)-dione (1.62 g, $0.1\,mol\,L^{-1}$) (for L^1 and L^2, respectively) was added dropwise with constant stirring at room temperature. The mixture was refluxed for 1 h and the solid was filtered and washed with dry methanol and then dried (figure 1). The elemental analysis data and melting points are given in table 1.

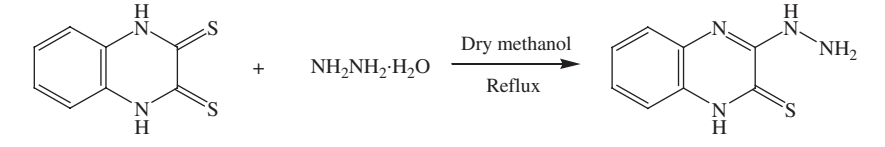

Quinoxaline-2,3(1,4H)-dithione Hydrazine hydrate 3-Hydrazinylquinoxaline-2(1H)-thione

Figure 2. Schematic representation of preparation of 3-hydrazinylquinoxaline-2-thione.

Table 1. Elemental analysis and molar conductivity data.

Compounds	Yield (%)	Color	m.p. (°C)	Elemental analysis (%) Found (calculated)						Molar conductivity Λ_M ($\Omega^{-1}cm^2mol^{-1}$)
				C	H	N	S	M	Cl	
L^1	86	Reddish brown	228–230	59.81(59.52)	3.40(3.52)	21.00(21.12)	9.96(10.08)	–	–	–
$[CoL^1Cl_2(H_2O)]$	74	Brown	>280	40.90(41.03)	2.76(2.83)	14.91(14.82)	6.81(6.72)	12.54(12.68)	15.12(15.04)	15.3
$[NiL^1Cl_2(H_2O)]$	78	Dark brown	>280	40.98(40.81)	2.77(2.69)	14.94(15.04)	6.83(6.73)	12.48(12.53)	15.15(15.21)	18.4
$[CuL^1Cl_2(H_2O)]$	80	Black	>280	40.54(40.63)	2.74(2.62)	14.78(14.81)	6.75(6.63)	13.41(13.58)	14.99(15.08)	17.1
$[ZnL^1Cl_2(H_2O)]$	76	Reddish brown	>280	40.37(40.30)	2.73(2.80)	14.72(14.72)	6.72(6.81)	13.77(13.86)	14.93(15.01)	14.3
L^2	84	Brown	241–243	57.14(57.20)	3.50(3.73)	25.00(25.14)	9.52(9.64)	–	–	–
$[CoL^2Cl_2(H_2O)]$	74	Dark brown	>280	39.67(39.72)	2.89(2.98)	17.35(17.28)	6.61(6.72)	12.17(12.26)	14.67(14.59)	16.4
$[NiL^2Cl_2(H_2O)]$	76	Dark brown	>280	39.71(39.80)	2.89(3.98)	17.37(17.42)	6.61(6.64)	12.09(12.18)	14.68(14.76)	15.6
$[CuL^2Cl_2(H_2O)]$	78	Black	>280	39.30(39.42)	2.86(2.79)	17.19(17.24)	6.55(6.44)	12.99(13.07)	14.53(14.67)	18.7
$[ZnL^2Cl_2(H_2O)]$	78	Brown	>280	39.14(39.22)	2.85(2.79)	17.12(17.06)	6.52(6.58)	13.35(13.47)	14.47(14.59)	15.7

2.2.3. Synthesis of complexes. Metal(II) chloride {$CoCl_2 \cdot 6H_2O$ (0.237 g, 0.01 mol L^{-1}), $NiCl_2 \cdot 6H_2O$ (0.237 g, 0.01 mol L^{-1}), $CuCl_2 \cdot 2H_2O$ (0.171 g, 0.01 mol L^{-1}), and $ZnCl_2$ (0.136 g, 0.01 mol L^{-1})} in EtOH (100 cm^3) was added with stirring to an ethanolic solution of ligand {L^1(0.314 g, 0.01 mol L^{-1}), L^2 (0.329 g, 0.01 mol L^{-1})} and refluxed at water bath temperature for 3–4 h. The solid complex obtained by this process was separated by filtration under suction, washed with hot ethanol, and then dried *in vacuo*.

3. Results and discussion

The transition metal complexes are non-hygroscopic (stable at room temperature) amorphous solids, soluble in dimethyl sulfoxide (DMSO) and DMF, sparingly soluble in ethanol and methanol, and insoluble in chlorinated hydrocarbons. The complexes melt with decomposition above 280°C. The elemental analysis data of the ligands and their complexes along with molar conductivity values are compiled in table 1.

3.1. *Molar conductivity measurements*

The molar conductance values of the complexes measured at room temperature in DMSO solution at 10^{-3} mol dm^{-3} fall in the range 14.3–18.7 Ω^{-1} cm^2 mol^{-1} (table 1) indicating nonelectrolytic nature of the complexes [14]. Comparatively high values are due to the solvation of DMSO, which replaces anions from the coordination sphere.

3.2. *IR spectral studies*

In both ligands, the amine ν(NH) absorptions are broad bands around 3180 cm^{-1} with a little shift and line broadening upon complexation. For L^1, an intense band at 1704 cm^{-1} is ascribed to the lactonic carbonyl group of isatin. Due to coordination of oxygen in complexes, a reduction of intensity and a shift in ν(C=O) is observed. For L^2, ν(C=O) is observed at 1681 cm^{-1} and experiences a negative shift upon complexation. The ν(C=N) observed at 1675 cm^{-1} in L^1 shifts to a lower frequency by ~10–20 cm^{-1} upon complexation due to coordination of azomethine nitrogen. In both ligands ring (C=N) stretching vibrations are observed around 1600 cm^{-1} and remain almost unaltered upon complexation. Thioamide bands having a major contribution from ν(C=S) are at 1293 and 767 cm^{-1} as sharp bands, which undergo considerable reduction in intensity and shift to lower frequency upon complexation, suggesting coordination of thione sulfur [15]. The low frequency non-ligand bands at 470 and 420 cm^{-1} are assigned to ν(M–N) and ν(M–S), respectively. The IR spectral data are provided in table 2.

3.3. *^{1}H-NMR studies*

^{1}H-NMR spectra of ligands and zinc complexes were analyzed. L^1 displays two singlets (D_2O exchangeable) at 11.91 and 11.02 ppm assigned to isatin and quinoxaline

Table 2. IR spectral data of ligands and complexes in cm^{-1}.

Compound	ν(OH) water	ν(NH)	ν(C=O)	ν(C=N)	ν(C=N) ring	Thioamide bands ν(C=S)		ν(M–N)	ν(M–S)
L^1	–	3180b 3182b	1704s	1675s	1613m	1293s	767s	–	–
$[CoL^1Cl_2(H_2O)]$	3417b	3250b	1715s	1662s	1617s	1284m	733m	472s	420m
$[NiL^1Cl_2(H_2O)]$	3407b	3176b	1713s	1665m	1614m	1283m	743m	465s	418m
$[CuL^1Cl_2(H_2O)]$	3439b	3200b	1686m	1651m	1614s	1277m	750m	471s	416s
$[ZnL^1\ Cl_2(H_2O)]$	3400b	3209b	1684m	1650m	1612s	1263m	753m	460s	417s
L^2H_2	–	3210b	1681s	–	1593s	1299s	815s	–	–
$[Co_2L_2^3\ (H_2O)_4]\cdot 2H_2O$	3416b	3200b	1650s	–	1550s	1251m	755m	493s	416s
$[Ni_2L_2^2\ (H_2O)_4]\cdot 2H_2O$	3417b	3216b	1646s	–	1548m	1251m	756m	486s	425s
$[Cu_2L_2^2\ (H_2O)_4]$	3422b	3200b	1652s	–	1598s	1250m	756m	471s	416m
$[Zn_2L_2^2\ (H_2O)_4]\cdot H_2O$	3442b	3220b	1669s	–	1556m	1252m	754m	470s	421s

s, sharp; m, medium; b, broad.

ring NH, respectively. They shift (12.13 and 10.99 ppm) upon complexation, suggesting coordination of oxygen and sulfur through ketone and thione. Hydrazine NH is observed at 8.53 ppm and shifts downfield in the respective zinc complex (9.01 ppm). The aromatic protons resonate in the range 6.61–7.58 ppm and undergo a little alteration in chemical shift value (6.80–8.04 ppm). The coordinated water resonates at 3.50 ppm and broadens the DMSO peak. In L^2, two singlets at 13.52 and 11.88 ppm were ascribed to ring NH of quinoxaline 2,3-(1,4H)-dione and 3-hydrazinyl quinoxaline 2-thione, respectively. In the zinc complex, they shift downfield (13.82 and 12.18 ppm) due to the variation in electron density and steric constraints brought about by chelation [16]. The hydrazine protons resonate at 9.50 ppm as doublet, suggesting their chemical equivalence. In the complex, since one NH participates in coordination, chemical equivalence is not maintained hence the peaks get separated. The coordinated NH shifts upfield at 10.00 ppm as doublet, whereas the non-coordinating NH is at 8.99 ppm. The aromatic protons (7.08–8.13 ppm) undergo a little change in chemical shift upon complexation (6.91–8.05 ppm) and coordinated water resonates at 3.50 ppm.

3.4. *Electronic spectral studies*

Electronic spectra of ligands and their complexes were recorded in DMF from 200–1000 nm. Both ligands exhibit similar electronic transitions with strong bands at 230–260 nm ($\varepsilon \sim 15{,}000\ L\,cm^{-1}\,mol^{-1}$), assigned to intraligand $\pi \rightarrow \pi^*$ transitions, which remain almost unchanged in the complexes. The transitions at 275–300 and 350 nm ($\varepsilon \sim 10{,}000\ L\,cm^{-1}\,mol^{-1}$) are assigned to $n \rightarrow \pi^*$ transitions of carbonyl and imine, respectively [17]; these peaks redshift upon complexation.

In all the complexes, an intense peak is observed at 400–420 nm with $\varepsilon \sim 30{,}000\ L\,cm^{-1}\,mol^{-1}$, assigned to ligand-to-metal CT transition (S → M) [17]. The cobalt(II) complexes show absorptions at 450 nm ($\varepsilon \sim 250\ L\,cm^{-1}mol^{-1}$), 570 nm ($\varepsilon \sim 200\ L\,cm^{-1}\,mol^{-1}$), and 830 nm ($\varepsilon \sim 150\ L\,cm^{-1}mol^{-1}$), assignable to d–d transitions, $^4T_{1g}(F) \rightarrow {}^4T_{1g}(P)$, $^4T_{1g} \rightarrow {}^4A_{2g}$, and $^4T_{1g}(F) \rightarrow {}^4T_{2g}$, respectively, evidencing octahedral complexes. In Ni(II) complexes, the lowest energy band at 860 nm

($\varepsilon \sim 150\,\mathrm{L\,cm^{-1}\,mol^{-1}}$) was due to $^3A_{2g} \rightarrow {}^3T_{2g}$ (ν_1) and bands near 600 nm ($\varepsilon \sim 200\,\mathrm{L\,cm^{-1}\,mol^{-1}}$), and 520 nm ($\varepsilon \sim 250\,\mathrm{L\,cm^{-1}\,mol^{-1}}$) were assigned to $^3A_{2g} \rightarrow {}^3T_{1g}$ (ν_2) and $^3A_{2g} \rightarrow {}^3T_{1g}(P)$ (ν_3), respectively. Appearance of these spin-allowed d–d bands indicates octahedral geometry around Ni [18]. Both Cu(II) complexes display closely spaced absorptions around 500 and 550 nm with low ε values ($\varepsilon \sim 100$–$120\,\mathrm{L\,cm^{-1}\,mol^{-1}}$), which are attributed to d–d transitions of d^9 system. Zn(II) complexes show only the absorptions around 420 nm ($\varepsilon \sim 15{,}000\,\mathrm{Lcm^{-1}\,mol^{-1}}$), corresponding to the intraligand transitions. The electronic spectral data of the ligands and their complexes along with the magnetic moment values are tabulated in "Supplementary material" (table S1).

3.5. *Magnetic properties*

The room temperature magnetic moment values of nickel and cobalt complexes were in the range 2.82–2.87 and 4.32–4.38 BM, respectively, suggesting the six-coordinate distorted octahedral geometry [19, 20]; copper complexes exhibit magnetic moment values (μ_{eff}) of 1.60–1.62 BM, which is subnormal even though there is no possibility of spin–spin interaction between the metal centers (since complexes are mononuclear). It is presumed that the higher covalency of Cu–S bond and low spin–orbit coupling of sulfur is responsible for the decrease in the effective magnetic moment values [21, 22].

3.6. *EPR spectral analysis*

Solid state X-band EPR spectra of the copper complexes exhibit isotropic intense broad signals with g_{iso} of 2.09 and 2.05. No hyperfine splitting in $g_{\parallel}$ or $g_{\perp}$ region and half-field absorption are observed. This type of spectrum was reported earlier for complexes bearing large organic ligand substituents having covalent metal–ligand bonds [22]. In this case, the higher covalency of sulfur–metal bond and the lower spin–orbit coupling of sulfur ligand may be the main factors affecting the EPR spectrum. The observations made in this study suggest the dependence of EPR parameters on coordinating atoms.

3.7. *Mass spectral analysis*

The spectral and analytical data suggest the empirical formula $[MLCl_2(H_2O)]$ for all the complexes (proposed structures are given in figure 3). The FAB mass spectral results are in agreement with the elemental analyses. The molecular formula $[MLCl_2(H_2O)]$ is hence assigned to all the complexes. In the mass spectra, the peaks at highest m/z value can be assigned for molecular mass with certainty, with the aid of consistent isotopic pattern. Hence, in this case, intense peaks at m/z 474 and 489 for Cu(II) complexes of L^1 and L^2 are consistent with the total molecular mass of the coordination complexes. Along with the molecular ion peak, spectra show some other peaks which are attributed to molecular cations of various fragments of complexes.

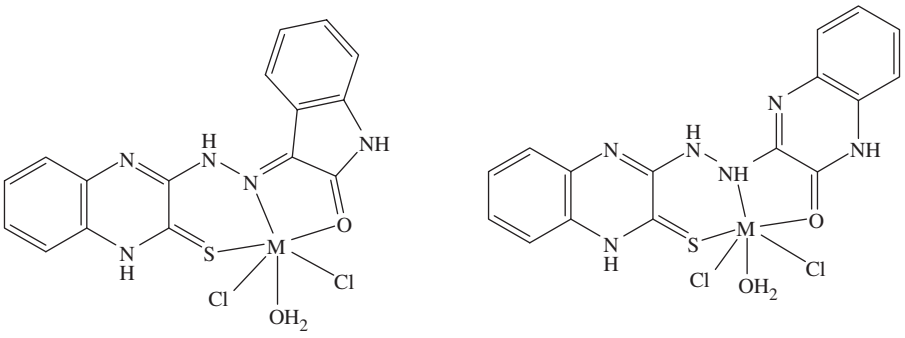

$[ML^1Cl_2(H_2O)]$ $[ML^2Cl_2(H_2O)]$

M = Co, Ni, Cu and Zn

Figure 3. Tentative structures for complexes.

3.8. *Thermal studies*

The thermal stability and decomposition pattern of the complexes was analyzed by TG and DTA studies in nitrogen with a heating rate of $10^{\circ}C\,min^{-1}$. Decomposition of $[CuL^1Cl_2(H_2O)]$ takes place in three stages. The first corresponding to a mass loss of ~3.80% at 100–140°C is attributed to loss of one coordinated water molecule. The corresponding differential peak (DTA) at ~120°C signifies an endothermic process. The second stage of decomposition is accompanied with liberation of two chlorides from 200 to 250°C with DTA curve at ~220°C representing an exothermic process. Further reduction of mass at higher temperature is ascribed to ligand decomposition. The final product was metal oxide. The copper complex $[CuL^2Cl_2(H_2O)]$ also exhibits a similar pattern of thermal decomposition with 3.68% weight loss at 150°C and 14.6% weight loss at 250°C corresponding to loss of one water molecule and two chlorides.

3.9. *Cyclic voltammetric studies*

The ligand and complexes ($0.001\,mol\,L^{-1}$ in DMSO) were scanned in the potential range −1.0 to 1.0 V in deareated conditions with different scan rates (0.05, 0.1, and $0.15\,V\,s^{-1}$). The copper and nickel complexes show redox reactions in the applied potential range, whereas the ligand and other complexes do not show electrochemical response, revealing that the redox property exhibited by copper and nickel complexes is purely metal based.

Both the copper complexes exhibit similar redox behavior. During the positive potential scan, the voltammograms display an anodic peak in the range $E_{pa} = 0.43$ to 0.55 V, which is assigned to oxidation of Cu(II) → Cu(III). The corresponding reverse scan shows one cathodic peak in the potential range $E_{pc} = 0.33$ to 0.41 V, attributable to subsequent reduction (Cu(III) → Cu(II)). The separation between cathodic and anodic peak potentials ($\Delta E_p = E_{pa} - E_{pc}$) for the redox couple Cu(II)/Cu(III) is greater than 60 mV, which indicates quasi-reversible redox process. Along with this, the dependence of peak potentials on scan rate and values of peak current ratio (I_{pc}/I_{pa}) (almost

constant but not unity) show quasi-reversible nature of the redox processes [23]. The nickel complexes of both ligands show almost the same electrochemical behavior, undergoing oxidation, Ni(II) → Ni(III), during the anodic scan (0.50–0.60 V), followed by the two cathodic peak potentials in the range 0.24–0.30 V and −0.45 to −0.55 V, attributed to two step reduction of Ni(III) species, Ni(III) → Ni(II), and Ni(II) → Ni(I). The redox couples Ni(II)/Ni(III) of both the nickel complexes exhibit the characteristic features of quasi-reversiblity similar to that of the corresponding copper complexes [23]. For reduction of Cu(II) (d^9) to Cu(I) (d^{10}), increase in the radius and change in configuration from square planar to tetrahedral is needed. On the other hand, Cu(III) (d^8) assumes square-planar geometry with a low-spin ground state and oxidation of Cu(II) to Cu(III) involves reduction in ionic radius [24]. The constrained cavity fit Cu(III) better and thus stabilizes the complex. The extra stability achieved by the complex on oxidation influence redox and slows down the rate of reduction. Detailed studies are required to understand the nature of chemical reactions following electron transfers which are helpful in enzyme catalysis. The representative voltammograms are given in "Supplementary material" (figure S4) and the numerical data in table S2.

4. Conclusion

Spectro-analytical investigation of the complexes reveals tridentate nature of the ligands with S, N, and O donors. In complexes of L^1, coordination occurs through quinoxaline thione group, azomethine nitrogen, and ketonic oxygen from isatin ring. L^2 coordinates through quinoxaline thione, hydrazine nitrogen, and ketonic oxygen of a second quinoxaline ring. In both cases, though different heterocyclic motifs are used to construct the ligands, the ligational behavior is almost the same and the SNO cavity fits transition metal(II) ions. The structural difference of ligands has no significant influence on the coordination behavior. The electrochemical behavior exhibited by copper and nickel complexes is assigned to redox of metal ion. These compounds can be used as structural and functional models for various metallobiosites. Detailed studies are required to analyze the utility of these compounds as biomimetics.

Acknowledgments

The authors thank the Department of Chemistry and USIC, Karnatak University, Dharwad for providing spectral and analytical facility. Recording of FAB mass spectra (CDRI, Lucknow) and ESR spectra (IIT, Mumbai) are gratefully acknowledged. The author, Naveen Kulkarni, thanks the Karnatak University, Dharwad for providing the Nilekani Research Scholarship.

References

[1] I. Pal, F. Basuli, S. Bhattacharya. *Proc. Indian Acad. Sci. (Chem. Sci.)*, **114**, 25 (2002).

[2] M. Sönmez, M.R. Bayram, M. Çeleb. *J. Coord. Chem.*, **62**, 2728 (2009).
[3] A. Rana, M. Sutradhar, S.S. Mandal, S. Ghosh. *J. Coord. Chem.*, **62**, 3522 (2009).
[4] N.R. Pramanik, S. Ghosh, T.K. Raychaudhuri, S.S. Mandal. *J. Coord. Chem.*, **62**, 3845 (2009).
[5] E.D. Brock, D.M. Lewis, T.I. Yousaf, H.H. Harper. Procter & Gamble Company, USA, World Patent WO 9951688 (1999).
[6] A. Gazit, H. App, G. McMahon, J. Chen, A. Levitzki, F.D. Bohmer. *J. Med. Chem.*, **39**, 2170 (1996).
[7] U. Sehlstedt, P. Aich, J. Bergman, H. Vallberg, B. Norden, A. Graslund. *J. Mol. Biol.*, **278**, 31 (1998).
[8] S. Dailey, J.W. Feast, R.J. Peace, I.C. Sage, S. Till, E.L. Wood. *J. Mater. Chem.*, **11**, 2238 (2001).
[9] T. Yamamoto, Z.H. Zhou, T. Kanbara, M. Shimura, K. Kizu, T. Maruyama, Y. Nakamura, T. Fukuda, B.L. Lee, N. Ooba, S. Tomaru, T. Kurihara, T. Kanno, K. Kubota, S. Sasaki. *J. Am. Chem. Soc.*, **118**, 10389 (1996).
[10] T. Yamamoto, B.L. Lee, H. Kokubo, H. Kishida, K. Hirota, T. Wakabayashi, H. Okamoto. *Macromol. Rapid Commun.*, **24**, 440 (2003).
[11] M.A. Philips. *J. Chem. Soc.*, 2397 (1928).
[12] L.J. Theriot, K.K. Ganguli, S. Kavarnos, I. Bemal. *J. Inorg. Nucl. Chem.*, **31**, 3133 (1969).
[13] A.I. Vogel. *Text Book of Quantitative Inorganic Analysis*, 3rd Edn, Longmans Green and Co. Ltd, London (1961).
[14] W.J. Geary. *Coord. Chem. Rev.*, **7**, 81 (1971).
[15] A.D. Naik, S.M. Annigeri, U.B. Gnagadharmath, V.K. Revankar, V.B. Mahale, V.K. Reddy. *Indian J. Chem.*, **41A**, 2046 (2002).
[16] R.M. Issa, S.A. Azim, A.M. Khedr, D.F. Draz. *J. Coord. Chem.*, **62**, 1859 (2009).
[17] A.B.P. Lever. *Inorganic Electronic Spectroscopy*, Elsevier Publishing Company, New York (1968).
[18] J.C. Bailar, H.J. Emeleus, R. Nyholm, A.F.T. Dickenson. *Comprehensive Inorganic Chemistry*, p. 3, Pergamon Press, Oxford (1975).
[19] A.E. Martell, M. Calvin. *Chemistry of the Metal Chelate Compounds*, p. 214, Prentice Hall, New York (1952).
[20] K.S. Abou-Melha. *J. Coord. Chem.*, **61**, 2053 (2008).
[21] N.V. Kulkarni, G.S. Hegde, G.S. Kurdekar, S. Budagumpi, M.P. Sathisha, V.K. Revankar. *Spectrosc. Lett.*, **43**, 235 (2010).
[22] E. Pereira, L. Gomes, B. Castro. *J. Chem. Soc., Dalton Trans.*, 629 (1998).
[23] C.L. Bailey, R.D. Bereman, D.P. Rillema. *Inorg. Chem.*, **25**, 3149 (1986).
[24] E.Q. Gao, W.M. Bu, G.M. Yaug, D.Z. Liao, Z.H. Jiang, S.P. Yan, G.L. Wang. *J. Chem. Soc., Dalton Trans.*, 1431 (2000).